Electronic Supplementary Information (ESI) for Journal of Materials Chemistry

A general route to nanostructured $M[V_3O_8]$ and $M_x[V_6O_{16}]$ (x = 1 and 2) and their first evaluation for building enzymatic third generation biosensors.†

Nathalie Steunou,* [a,b] Christine Mousty,[c] Olivier Durupthy,[a] Cécile Roux,[a] Guillaume Laurent,[a] Corine Simonnet-Jégat,[b] Jacky Vigneron,[b] Arnaud Etcheberry,[b] Christian Bonhomme,[a] Jacques Livage,[a] and Thibaud Coradin.[a]

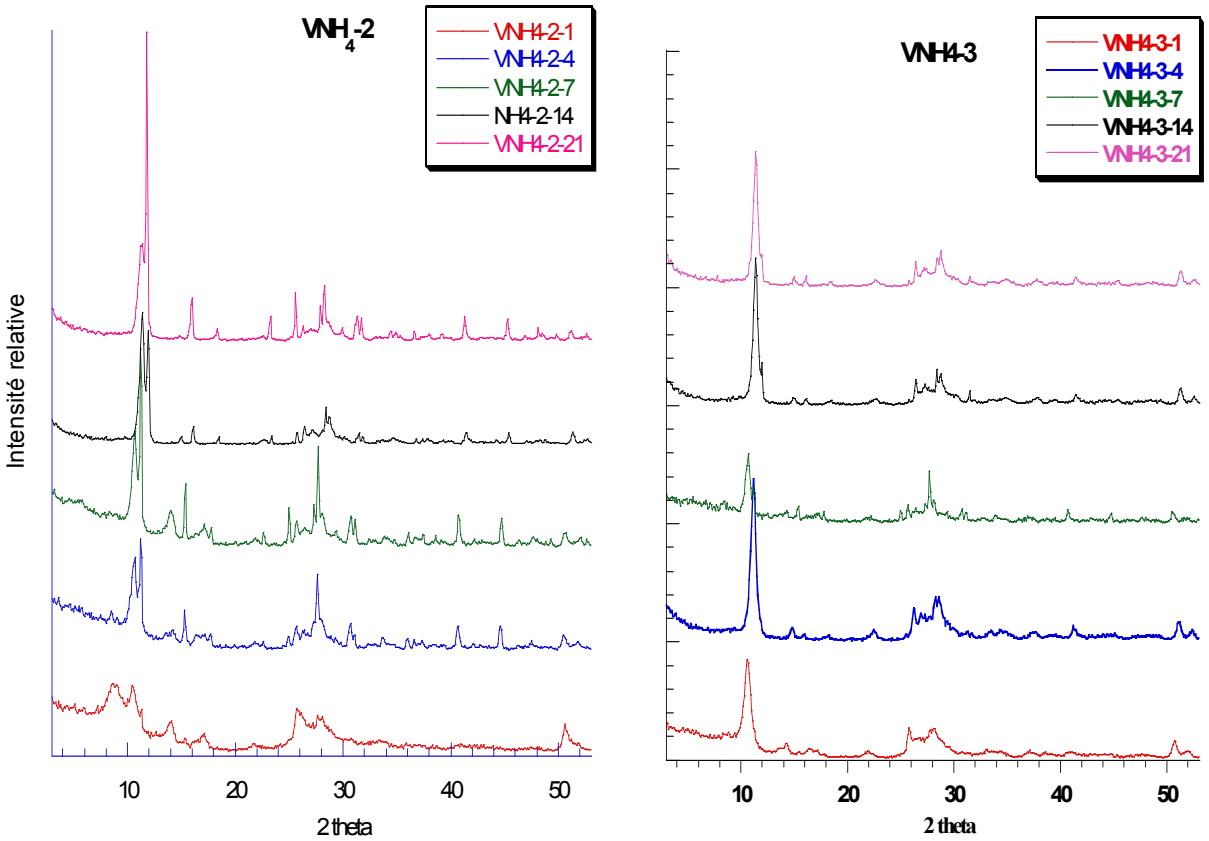

Fig. S1: X-ray diffraction patterns of $M[V_3O_8]$ and $M[V_6O_{16}]$ phases. In the title of figures VM-X-Y, M corresponds to the cation, X to the pH value and Y to the ageing time.

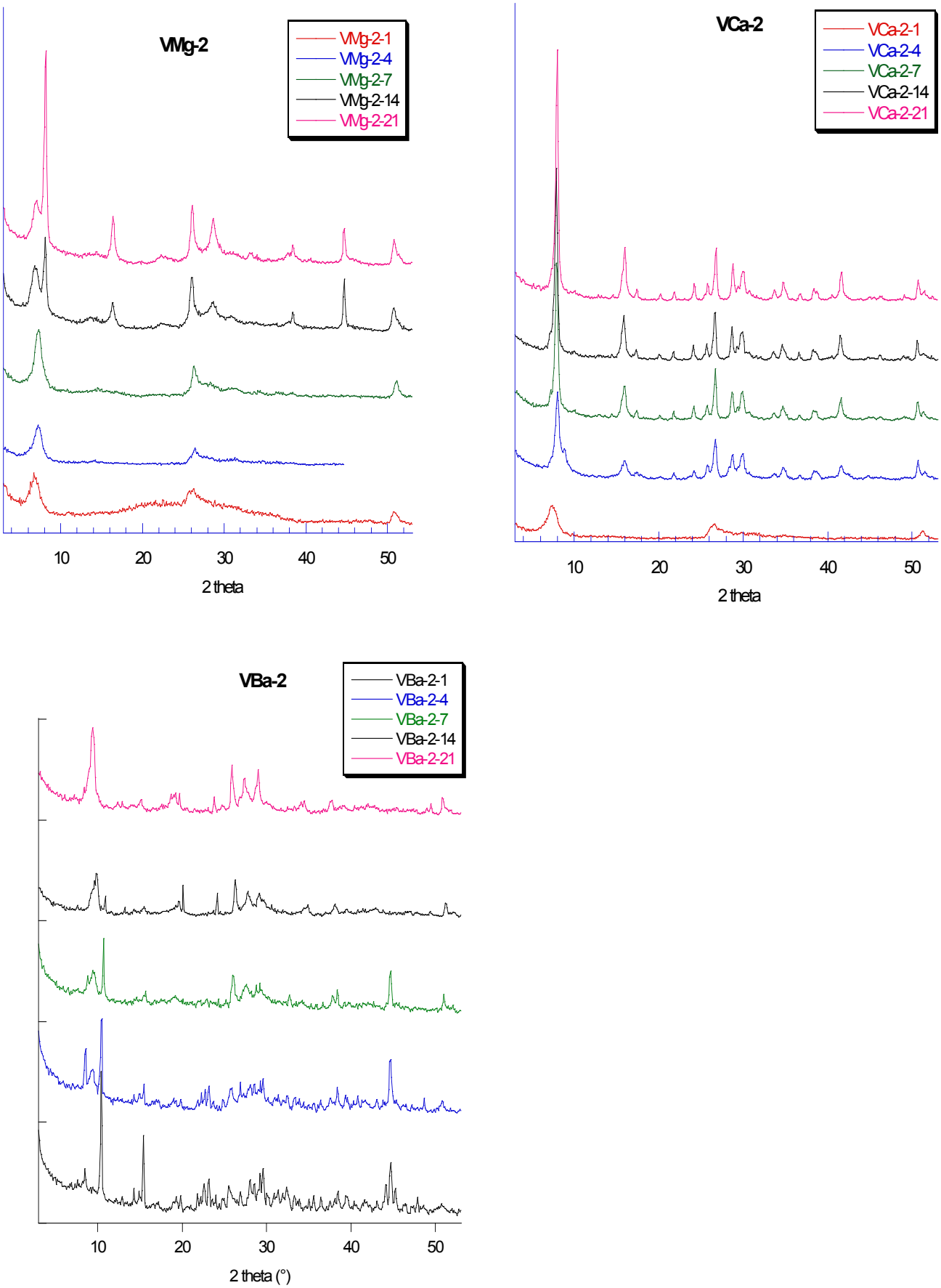

Fig. S1: X-ray diffraction patterns of M[V_3O_8] and M[V_6O_{16}] phases. In the title of figures VM-X-Y, M corresponds to the cation, X to the pH value and Y to the ageing time.

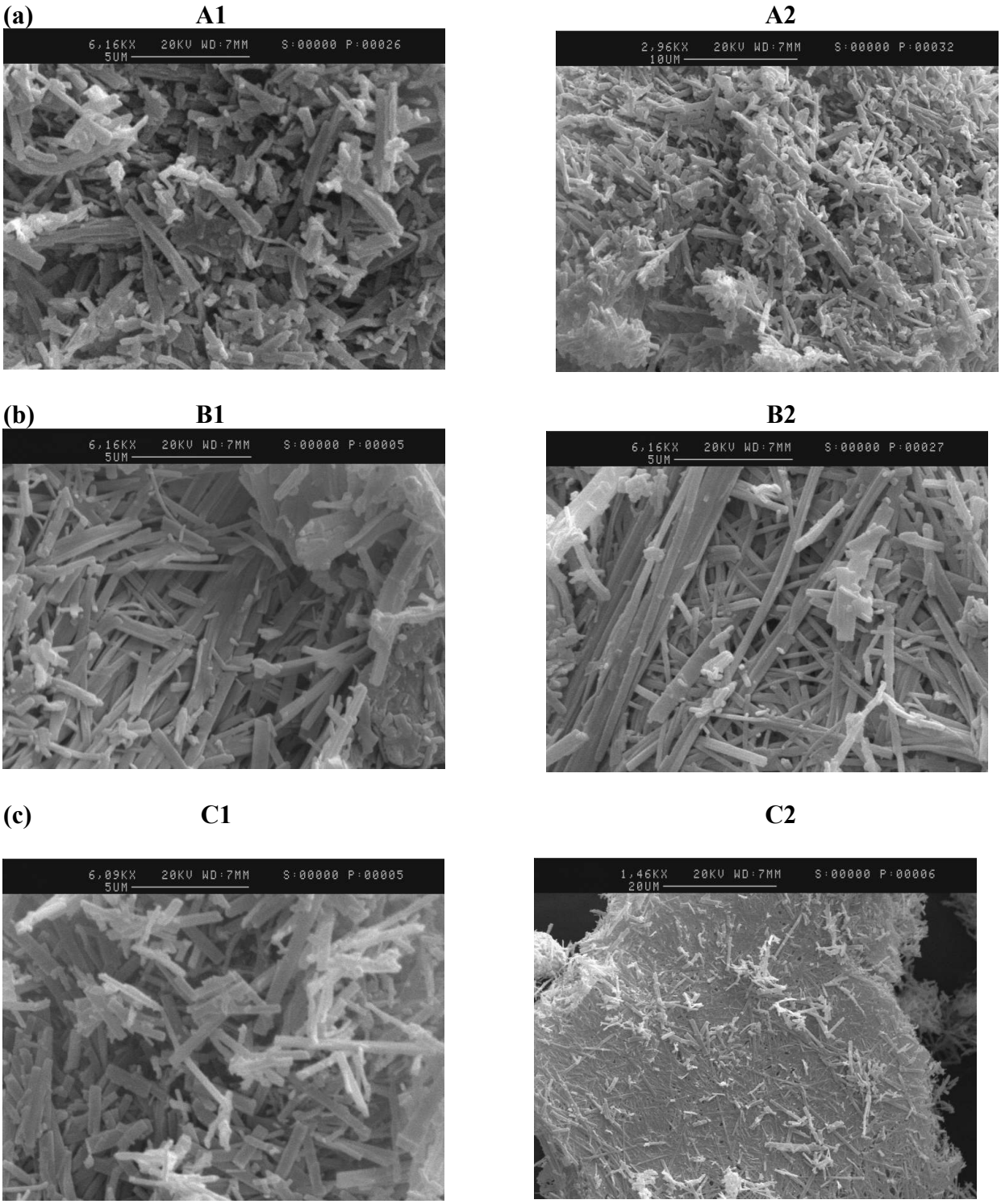

Fig. S2: SEM images for (a) $Mg[V_6O_{16}]7.1H_2O$ (images A1 and A2, pH_i = 2, 4 days); (b) $Ca[V_6O_{16}]\ 9.7H_2O$ (image B1 pH_i=2, 7 days) (image B2 pH_i = 3, 14 days) ; (c) $Ba_{1.2}[V_6O_{16}]5.5H_2O$ (images C1 and C2, pH_i =2, 14 days)

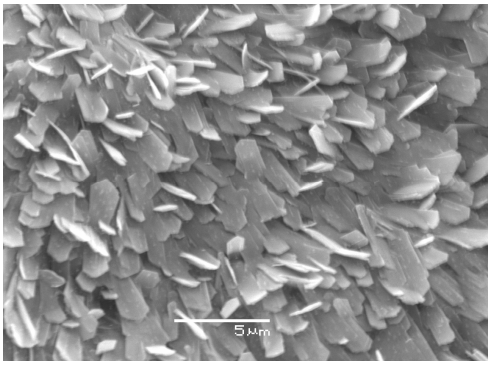

Fig S3. SEM images of $K_2[V_6O_{16}]$ -GOx biomembrane prepared by adsorption.

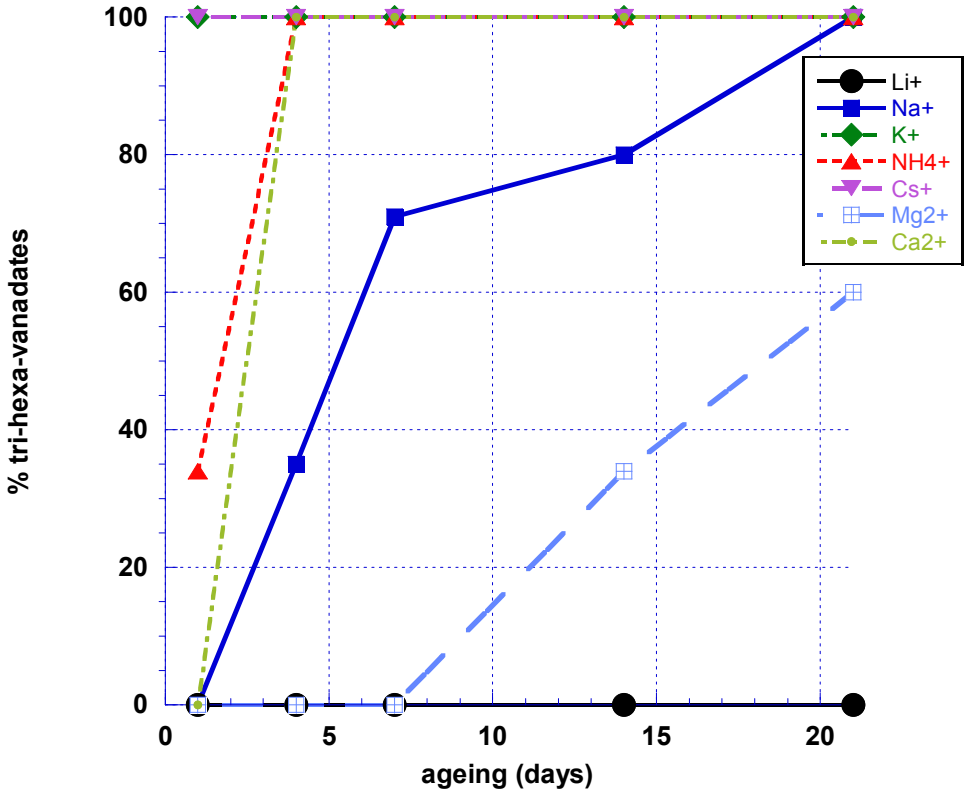

Fig S4: Relative amount of tri- and hexavanadates (i. e. m (MV_3O_8/(m(MV_3O_8)+ m(V_2O_5)) versus ageing at pH 2 for different monovalent and bivalent cations. The relative amount of $Ba_{1.2}[V_6O_{16}]$ is not reported because of the concomitant presence of $3Ba[V_{10}O_{28}]21H_2O$ in a significant amount.

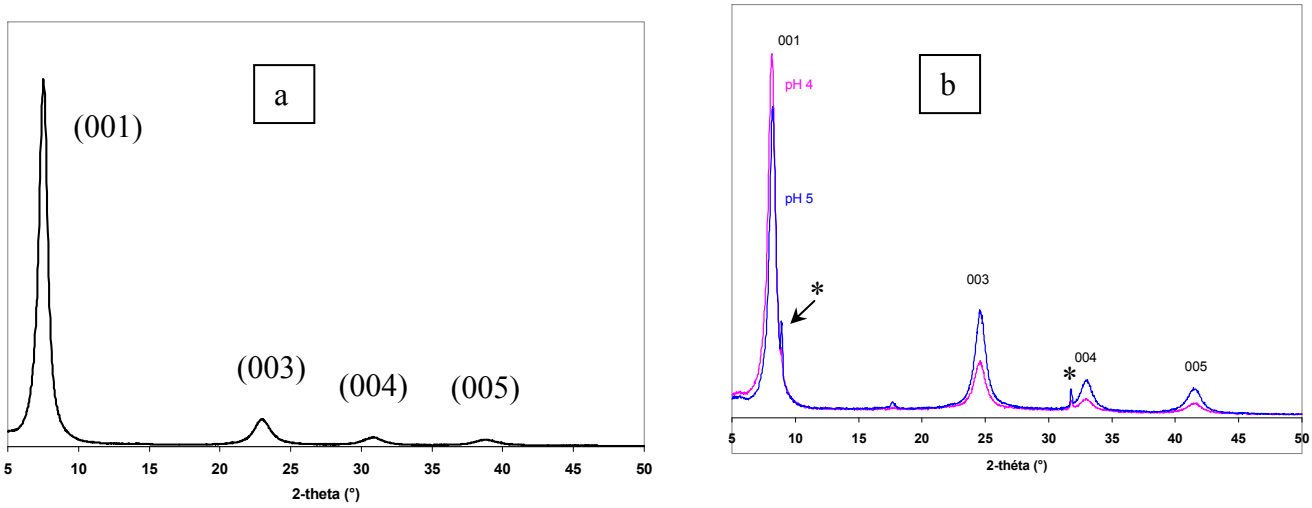

Fig. S5. XRD pattern of (a) $V_2O_5.nH_2O$ gel at pH 1, (b) $V_2O_5.nH_2O$ gel at pH 4 and 5.

For these experiments, $V_2O_5.nH_2O$ gels are deposited on glass substrates and the resulting films are immersed in acetate buffers of pH between 3 and 5. Due to the preferential orientation of V_2O_5 ribbon particles on flat surfaces, the XRD pattern of $V_2O_5.nH_2O$ gels at pH between 1 and 5 display only the series of 00ℓ reflections. The XRD diagrams of $V_2O_5.nH_2O$ gels at 3<pH<5 indicate that the structure of the gels is preserved until pH 5 despite of a little difference in the d_{001} value indicating a slight modification of the interlamellar space and the presence of an impurity of small amount at pH 5 (*).

The XRD pattern of V_2O_5 sol at pH 5 and $V_2O_5.nH_2O$-GOx biomembranes do not display XRD reflections. Actually, by redispersion of the gel in aqueous solution, the resulting V_2O_5 sol is then deposited on the glass substrate and dried. The stacking of V_2O_5 particles is not anymore present in the dried V_2O_5 film and the particles are completely disorganized. Since V_2O_5-GOx biomembrane results from the adsorption of enzyme onto these V_2O_5 films, no XRD reflections are present in the pattern of the $V_2O_5.nH_2O$-GOx biomembranes.

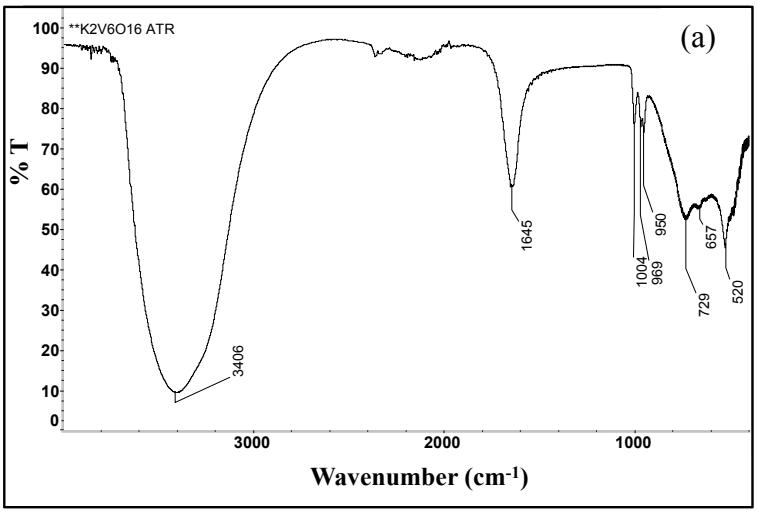

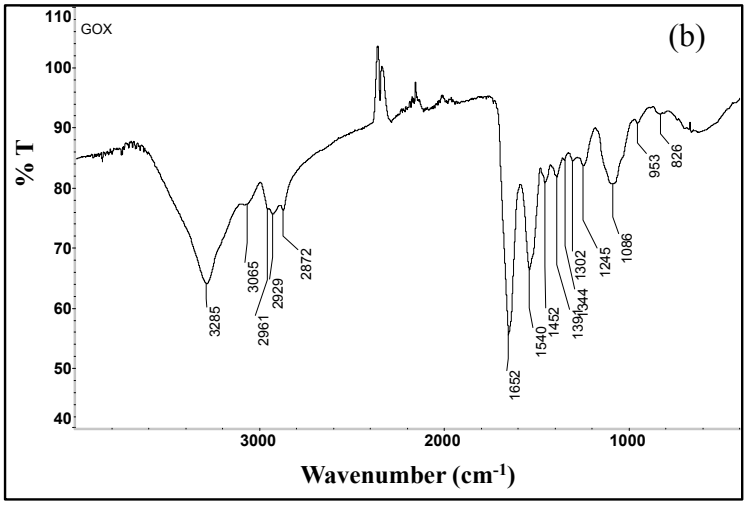

Fig. S6. Representative FT-IR spectra of pure a) $K_2[V_6O_{16}].nH_2O$ and b) GOx samples.

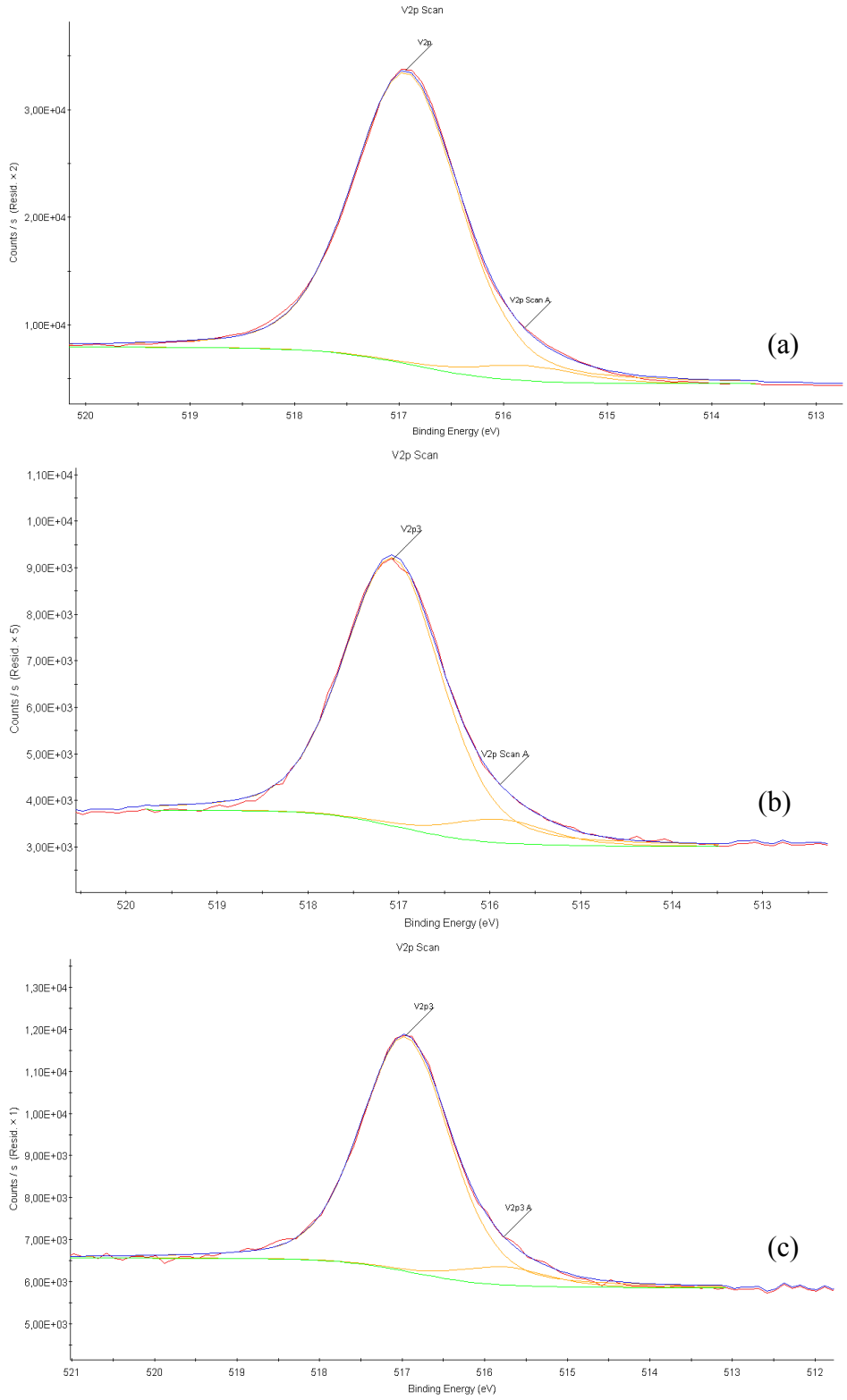

Fig. S7. V2p3/2 XPS spectra of a) $K_2[V_6O_{16}]$- pH 3, b) $K_2[V_6O_{16}]$- pH 6) c) $K_2[V_6O_{16}]$-GOx_{cos}

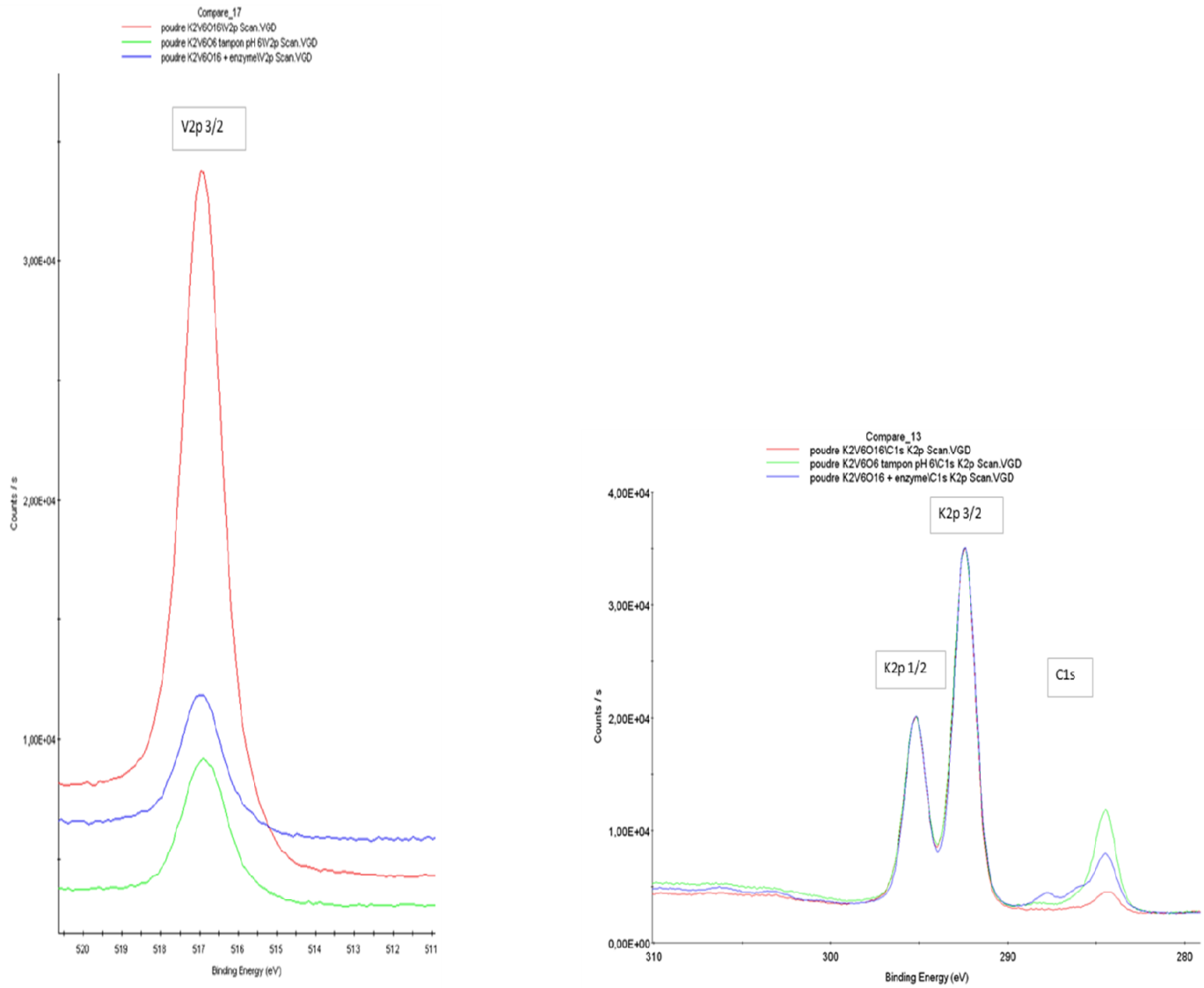

Fig. S8. Comparison of a) the V2p , b) K2p and C1s XPS spectra for $K_2[V_6O_{16}]$-pH 3, $K_2[V_6O_{16}]$-pH 6) and $K_2[V_6O_{16}]$-GOx_{cos}

Table S1. V2p 3/2 peak positions and atomic ratio for $K_2[V_6O_{16}]$-pH 3, $K_2[V_6O_{16}]$-pH 6) and $K_2[V_6O_{16}]$-GOx_{cos}

sample	Positions (eV)	Assignment	FWHM (eV)	Area (P) CPS.eV	%	$[V^{5+}]/[V^{4+}]$
$K_2[V_6O_{16}]$-pH 3	515.79 516.93	V2p Scan A (V^{4+}) V2p (V^{5+})	1.21 1.21	2028.43 39416.73	0.27 5.24	19.4
$K_2[V_6O_{16}]$-pH 6	515.89 517.07	V2p Scan A (V^{4+}) V2p3 (V^{5+})	1.28 1.28	767.73 8769.83	0.13 2.17	16.7
$K_2[V_6O_{16}]$-GOx_{cos}	515.77 516.96	V2p 3A (V^{4+}) V2p3 (V^{5+})	1.27 1.27	653.64 8519.45	0.11 1.38	12.5

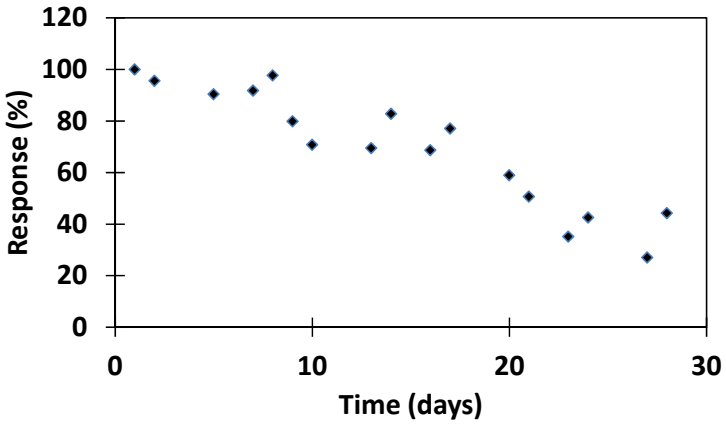

Fig. S9. Storage stability of the $K_2[V_6O_{16}]$-GOx_{cos} biosensor (pH 6.0)